XRF MICRO-ELEMENTAL STUDY OF ACCRETED ICE FROM LAKE VOSTOK

M. de Angelis[1], M. Fourcade[1], J.M. Barnola[1], J. Susini[2] and G. Durand[1]

[1] LGGE, BP96, 38402 St Martin d'Hères, France, [2] ESRF, BP 220 38043 Grenoble, France

Abstract

X-Ray micro-fluorescence studies of three samples taken along accreted ice from Lake Vostok at 3539, 3551 and 3572 m, were performed using the European Synchrotron Radiation Facility in Grenoble. The first sample (3539 m) was made of very clean ice without visible inclusion, the two other samples contained visible inclusions of various size. One crystalline structure, possibly a grain boundary, was observed in the sample taken at 3551 m. Based on ionic chromatography analyses, the 3539 m deep sample had a total ionic content lower than 10 ng g^{-1}, while high NaCl concentrations (Cl ~1000 ng g^{-1}) and large, although rather different, amounts of sulfate salts were found in the two other samples. In the conditions of our experiment, the μXRF technique allows to make 2D elemental maps of the sample surface for elements lighter than Ca.

Clear ice contained very few and small bubble-shaped inclusions with well mixed very thin mineral particles or salts inside. In inclusion-rich ice, three types of features were observed : i) Fine (3 to 15 μm in diameter) and oblong brine droplets, probably water pockets containing lake water mixed with halite rich hydrothermal water. These droplets were very likely in liquid state before the ice was extracted and are rather regularly distributed on a submillimetric scale. ii) Scattered, large and irregular aggregates of solid particles containing a mixture of very fine minerals, namely alumino-silicate, carbonate, sulfate salts and other sulfur and silicate specie. iii) A grain-boundary structure which seemed to gather only few small particles, salt or insoluble dust, confirming that most impurities are sequestred inside large crystals having slowly grown, once the ice was formed.

These results support the preliminary conclusions deduced from macroscopic chemical measurements by de Angelis et al. (2004), and provide useful information on mechanisms driving ice accretion.

Introduction

The largest subglacial lake identified under the Antarctic ice cap is Lake Vostok [1, 2]. The lake is 230 km long and 50 km wide. Evidence from water isotope studies and ice properties such as crystal sizes, electrical conductivity and total gas content show that the deeper part of the Vostok ice core is made of two distinct types of ice separated by a sharp transition. Above 3538 m depth, the ice is meteoric, originating from the ice sheet, while below 3539 m it originates from accretion, i.e. refreezing of the lake water [3]. Accretion ice is made of large ice crystals of very high crystalline quality similar to that of single crystals carefully grown under laboratory conditions [4]. Two main types of accreted ice may be distinguished : in the upper part, the ice (accretion ice-1) contains many visible inclusions, mainly located between 3540 and 3608 m depth [3]. Below 3608 m, the ice is clear, without visible inclusions (accretion ice-2). Two other thin layers of ice containing no or very few visible inclusions (ice-2 type), are observed : the first is located just below the glacier ice (3538-3553) and the second from 3588 to 3594 m depth.

The first comprehensive study of the ionic composition of accretion ice was made by de Angelis et al., [5]. These authors have shown that accretion ice is significantly different in composition from glacier ice. Large and varying concentrations of salts, dominated by halite and calcium or magnesium sulfate, are observed in accretion ice. Some of these salts are homogeneously distributed throughout the ice lattice (halite, fluoride and nitrate), while the remaining (sulfate and ammonium salts) seem to be preferentially located in scattered solid inclusions or, to a lesser extent, at grain boundaries. Up to now, very little is known concerning these visible inclusions, mostly because they vanish when samples are melted. Only preliminary studies of their insoluble part have been carried out by optical microscopy and show that some contain

fine particles (clays or quartz, and dust of unidentified origin). The study of de Angelis et al.[5] allows to conclude that they contain sulfate salts

From chemical considerations supported by additional isotopic and Fe measurements, and considering the possible geological history of Lake Vostok and the bottom topography [6], these authors proposed that these salts originate from deeper sedimentary strata, close to evaporites in composition. They also concluded that inclusion-rich and salty ice likely forms in the shallow bay upstream from Vostok on the northeastern side of the lake, while ice without visible inclusion, containing very few impurities, forms when the glacier passes over the deep main lake.

This paper present an attempt to check the scenario proposed by de Angelis et al., and based on macroscopic studies. A quite new technique allowing the non destructive and in situ analysis of ice samples was used, with the aim to understand where impurities were localized in accreted ice, and what they were made from.

Method and sampling

The method, based on XRF microprobe technique developed at the ID21 beam-line of the ESRF is described in detail in Fourcade et al. [7] . The localization of impurities in the ppm range and the individual mapping of elements lighter than Ca is possible using this technique, which makes also possible elemental speciation, mainly of sulfur species. For that to do, the beam intensity is focused on sulfur energy (2.5 keV) instead of Ca energy (4.5 keV). A specific cryo-system was used [8] to maintain the cell containing the sample at – 140°C under high vacuum (2.10^{-5} kPa), during X-Ray micro-scanning which took up to several hours. This system allowed to study the upper 50 µm of ice samples, 1 cm in diameter and 5 mm thick, without visual change of the ice suface. A first examination of the sample was made using an optical microscopy equipment coupled with the XRF microprobe.

Samples were prepared in the cold room facilities of the LGGE in Grenoble. Every ice section (roughly 2 x 2 x 4 cm) was fixed with a drop of freezing water on the bottom of a sample cell. The outer part of the sample was removed using a lathe, until its diameter corresponded to the cell inner diameter, then the sample was cut lengthwise with a band saw and shaved with a microtome to a final thickness corresponding to the cell height. As previously tested by Legrand et al. [9], such mechanical procedure is also very efficient for contamination removing. To avoid sample sublimation under high vacuum, the cell was tightly closed with a film of ultralene [8].

Table 1

Ionic composition of accretion ice. Grey area correspond to ice layer without visible inclusion (ice-2). For every depth, concentrations were measured in a sample taken in the same ice section as the corresponding sample presented in this study and very close to it. Eye visible patterns (EVP) to be examined by XRF analysis, if any, are indicated (GB grain boundary, GI giant inclusion), as well as the beam energy. When centered at 2.5 keV, the beam energy allows to study sulfur speciation, but elemental mapping are limited to elements with atomic weight equal to or lighter than S.

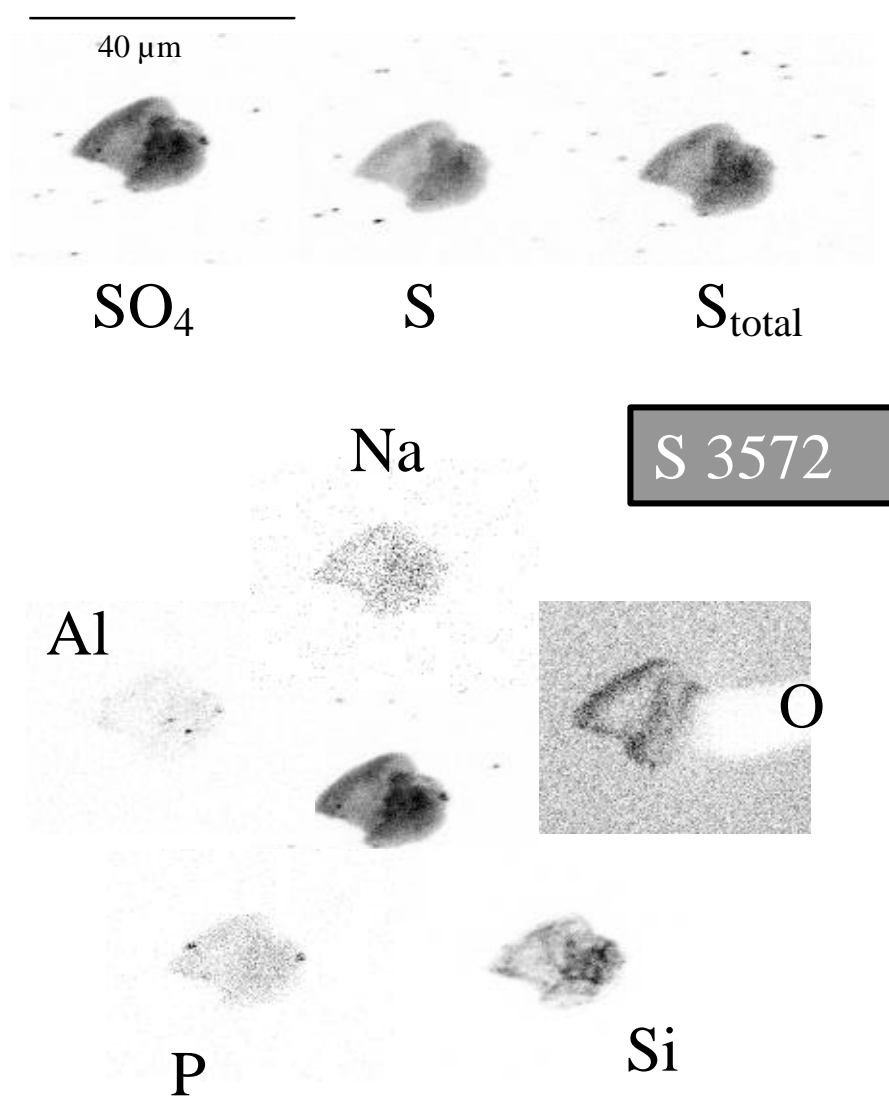| Sample	Depth	F-	MSA	Cl-	NO_3^-	SO_4^-	Na^+	NH_4^+	K^+	$Mg2^+$	Ca^{2+}	EVP	Beam Energy
	(m)					Concentrations are in ng g^{-1}							keV
S 3539	3539	.063	0.00	2.2	1.06	0.87	1.90	0.21	0.35	0.22	0.92		4.5
S 3551-a	3551	3.13	0.00	938	1.73	215	798	1.71	5.01	0.71	94.9	GB	4.5
S 3551-b												GI	4.5
S 3572	3572	2.33	0.00	721	2.10	44.5	623	3.08	9.31	5.47	25.2		2.5

Considering NaCl and Ca- $MgSO_4$ profiles [5] and typical visible patterns (inclusion, grain boundary), several accretion ice samples were prepared, but only four of them were examined during this prospective study : the first one (S 3359) was taken at 3539 m depth, in the upper layer of ice-2, where ionic content was extremely low and very close to what can be measured in ultrapure water. The three others were taken in ice-1,

two at 3551 m and one at 3572 m, were large peaks of sulfate salts and many inclusions were observed; A thin structure, likely a sub-grain boundary was clearly visible in the first sample at 3551 m (S 3551-a), and it was possible to prepare another sample from the same level with a very large inclusion (~800 µm) near the surface (S 3551-b). Nothing typical was visible in sample at 3572m (S 3572), except few fine inclusions.

Figure 1: Elemental mapping of an inclusion at 3572 m. The scanning resolution is 0.3 µm. The relative abundance of a given element in a given pixel is directly related to the signal intensity measured in the considered pixel, which increases from white to black. In every elemental mapping, the highest concentration is automatically scaled to dark.

The ionic composition of these four samples is reported in Table 1, along with eye visible patterns observed, if any, and XRF micro-analysis conditions. The first sample to be analyzed was S 3572. The beam energy was centered at 2.5 keV for sulfur speciation, preventing to study elements heavier than S (i.e. Cl, K and Ca). Later on (S 3539, S 3551-a and -b), the beam energy was centered at 4.5 keV.
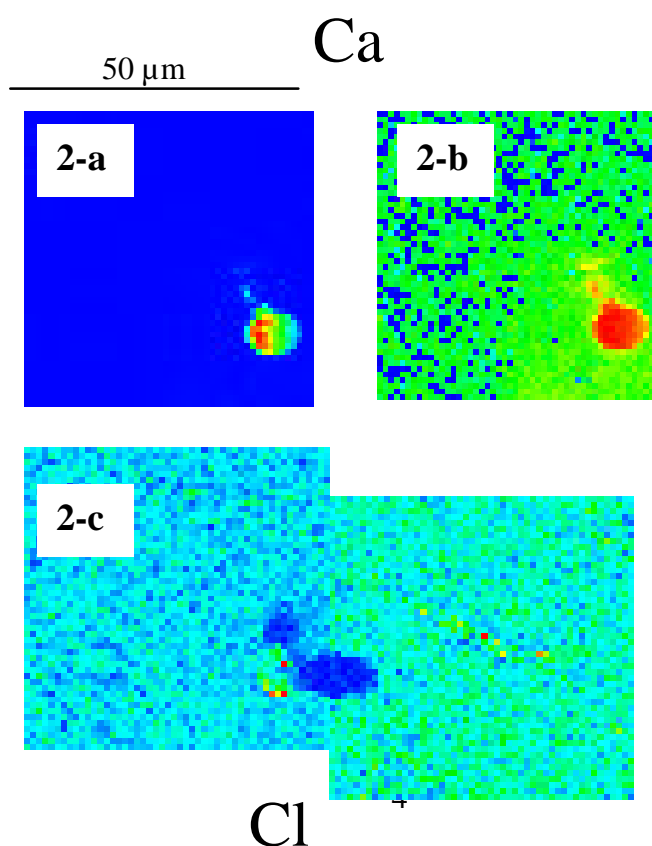
Results

µXRF investigations were focused on objects previously spotted by optical microscopy (grain boundary, inclusions, matrix irregularities), or made by scanning selected areas for background studies. The study presented here was not exhaustive for two main reasons : i) the poor quality of optical microscope imaging did not allow to identify all interesting objects ii) scanning areas of a few µm^2 took several hours and the time allocated for this prospective experiment was short (2 days). It must also be emphasized that 2D mapping allows to identify elements having the same localization and thus, potentially associated. However, the sensitivity for a given element strongly decreases with its atomic weight, preventing to discuss quantitative relationships between elements not very close in energy.

Sulfur speciation

S 3572 : Despite the surface shape of this sample was probably tilted making very hard preliminary investigation by optical microscopy, several sulfur rich and rather large objects were spotted by nightly scanning and more thoroughly examined later. One of these object is shown in Fig.1. Both reduced and oxidized forms of sulfur are observed, with rather different localization. Lighter elements are also present, in particular Si, Al and O. Its elemental mapping suggests that this object is made of aggregated finer particles including alumino-silicates, sulfate salts and sulfur species. One interesting feature is the apparent lack of Oxygen in ice lattice (white area in O mapping of Fig. 1), possibly due to beam shadowing by the particle.

Figure 2: Bubble shaped object at 3539 m. The resolution is 0.5 µm. The relative abundance of a given element in a given pixel is directly related to the signal intensity measured in the considered pixel, which increases from dark blue to red. In every elemental mapping, the highest concentration is automatically represented by a red pixel. This object contains fine mineral particles shown on the Ca mapping (2-a linear intensity scale, and 2-b logarithmic scale) and Cl diluted solution (2-c). A tail like prolongation is clearly visible when using the logarithmic scaling.

Normal condition

S 3539 : As expected, this sample appeared very clean: no particle were identified by preliminary optical microsopy and the matrix composition (dominated by Cl) was not significantly different from a synthetic sample of ultrapure frozen water [7]. Very few thin particles were detected The largest one, round-shaped and ~10 μm in diameter, is shown in Fig.2. The elemental mapping of this particle suggests that it contains not only aluminosilicate and sulfur species but also Cl probably present as NaCl. Its form is very different from particles observed in S 3572 and will be discussed in the following section. As for O in S 3572, a shadow-like feature is observed for Cl. This may be due the presence of small amount of Cl present as a solid solution in ice lattice and/or to a possible artefact by the ultralene film [7]
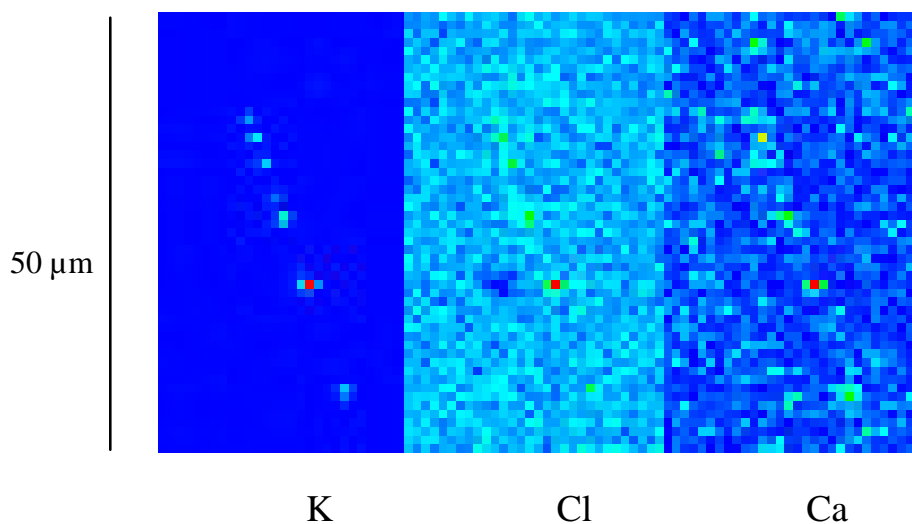
S 3551-a : as shown in Fig.3, very few small particles, in the μm range, were observed along the sub-grain boundary structure. K, Cl and Ca are quite visible. As previously observed, a shadow is visible on Cl mapping. The possible presence of Cl in ice lattice is supported by background intensity values slightly higher (25 ± 8 in arbitrary units) in

this sample than in the ultrapure reference sample (10 ± 3).

S 3551-b : This sample contained a giant inclusion (~800 μm), the detailed composition of which will be presented elsewhere. As shown in Fig. 4, this inclusion is a quite heterogeneous mixture including smooth and round carbonate-rich particles (Fig.4-c) and a wide range of other particles with various shapes and compositions, among which fine alumino-silicate (Fig.4-d) and larger aggregates of sulfate (Fig.4-a), associated to magnesium (Fig.4-b) and containing significant amounts of K and Si (Fig.4-d).

Beside this giant inclusion and other scarce and smaller aggregates, few colorless and oblong objects, rather regularly scattered where spotted by optical microscopy. Five of them were observed over an area of 200 x 200 μm^2, with apparent diameter varying from ~ 3 to ~ 15 μm. They are presented in Fig.5. Probably due to heating by microscope lamp, the first we attempted to examine explosed (Fig.5-e). All these objects are bubble shaped and depict very similar elemental composition.

Figure 3 : Grain boundary at 3551m. The relative abundance of a given element in a given pixel is directly related to the signal intensity measured in the considered pixel, which increases from dark blue to red. In every elemental mapping, the highest concentration is automatically represented by a red pixel. The resolution is 1 μm.
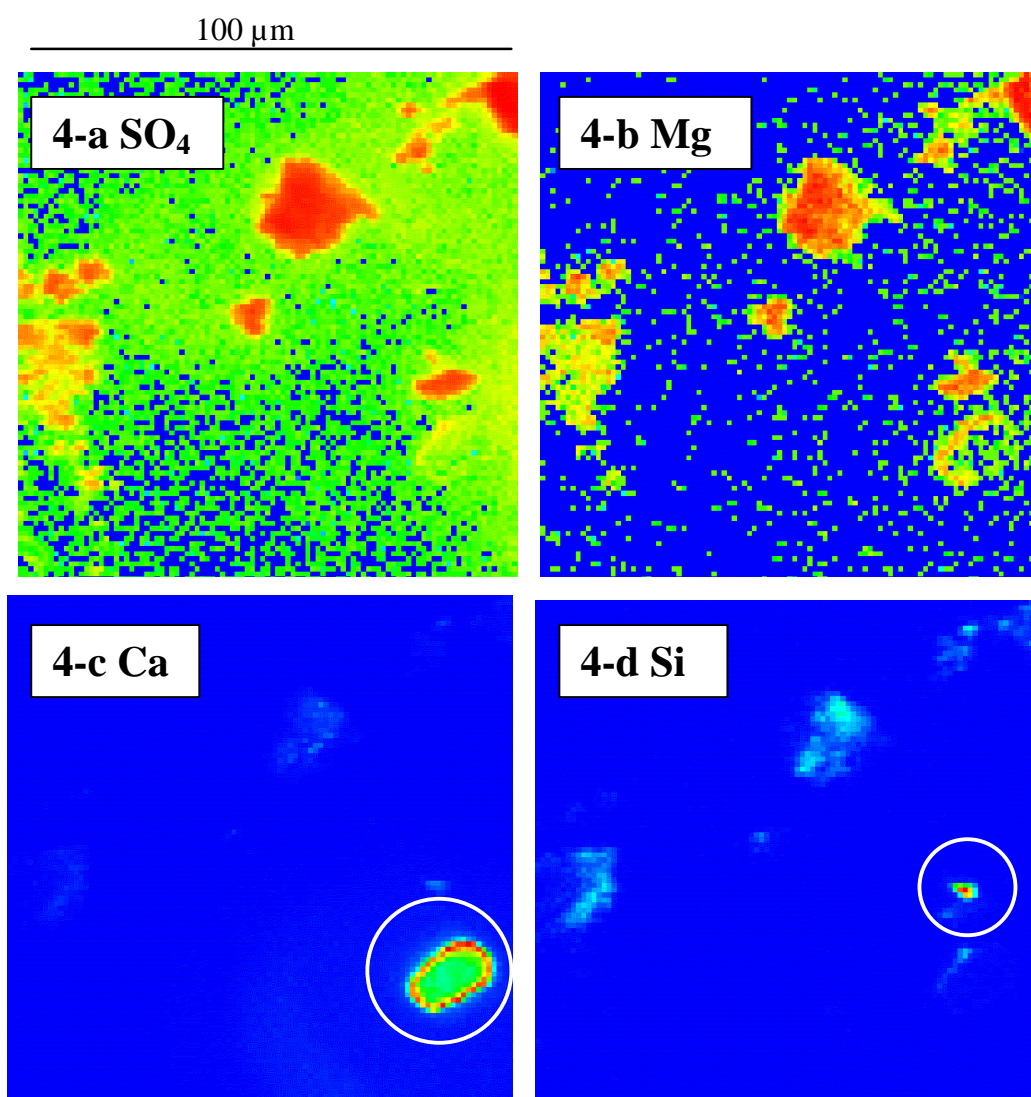

50 μm

K   Cl   Ca

S 3551-a

Their energy spectrum is largely dominated by Cl with smaller, although visible Na and K peaks. Significant amounts of other elements were not observed. Considering the sharp decrease of elemental response with energy [8], we can co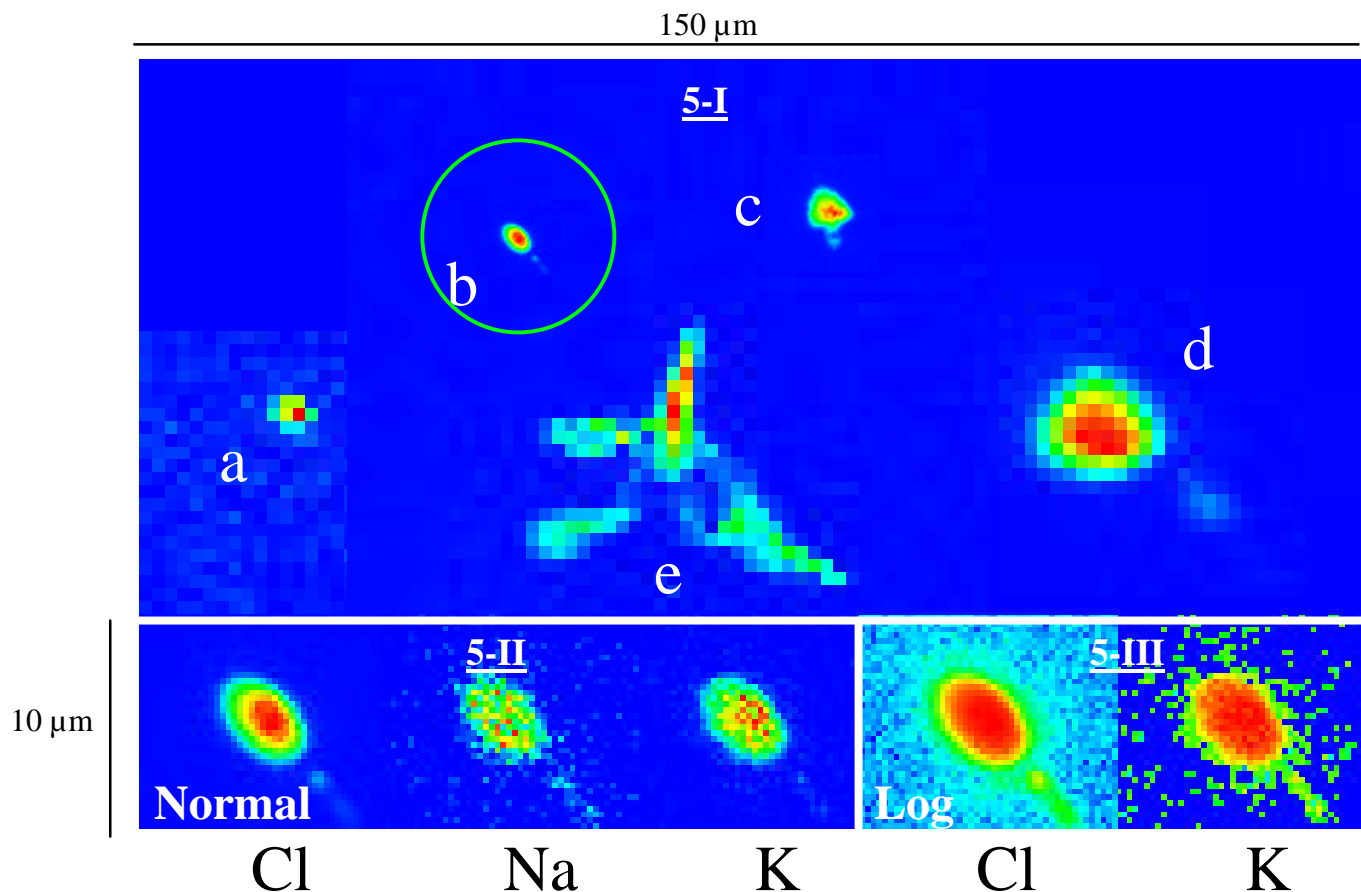nclude that Na concentrations are also high, while the contribution of K remains of minor importance. As shown in the lower part of Fig.5, concentrations decrease from the outer to the inner part of the bubbles and all of them are prolonged by a thinner tail-shaped feature. Interestingly, the shape of the particle observed in ice-2 (S 3539, Fig.1) is very similar.

Figure 4 : Exemple of particles observed on the border of the giant inclusion at 3551 m. The resolution is 1 µm. Intensity increases from dark blue to red. Due to the exponential decrease of elemental sensitivity with atomic number, SO$_4$ (4-a) and Mg (4-b) mapping are made using a logarithmic intensity scale. Round shaped carbonate and finer alumino-silicate particles, shown by white circles (4-c and 4-d, respectively) are also visible.

S 3551-

Figure 5 : Brine inclusions at 3551 m. Intensity increases from dark blue to red. Several images have been put together in the upper part of the figure (a, b, c, d, e) allowing to compare elemental distributions as well as particle shapes and sizes. The resolution varies from 0.3 µm (-b and –c) to 1 µm (-a, -d, and –e). Particle e has exploded (see text). Particle b is zoomed in the lower part of the figure (5-II). The tail-shaped feature observed for all brine bubbles (Fig.-I), is clearly visible on the logarithmic representation of Cl and K mapping (Fig.5-III).

Discussion

This preliminary study clearly shows that a large part of the impurities present in accreted ice-1 are gathered in large and scattered inclusions. These inclusions contain a mixture of various and thinner particles, among them alumino-silicates and carbonates, sulfur compounds and other silicate species. The existence of sulfate salts proposed by de Angelis et al. [5] is confirmed, but significant amounts of other sulfur forms have been observed (S 3572) suggesting that inclusions may also contain fine debris of pyrite. The presence of quartz or amorphous silica produced by in situ reactions may explain that Si is not necessarily associated to Al. Nothing can be inferred from this study concerning the particle solubility, but the heterogeneity of the inclusions where they are collected strongly suggests that they were in solid state when accretion ice formed.

Inclusions do not contain noticeable amounts of Cl compounds, while NaCl concentrations as high as 1.5 µg g^{-1} were

measured in ice-1 (Table 1). Although a small quantity of Cl may be present as solid solution in ice lattice, it was almost exclusively detected in bubble like structures, where it is associated to large amount of Na and a smaller contribution of K. These objects are very likely brine micro-pockets entrapped in ice lattice. Our study supports the conclusion of De Angelis et al.[5]: fine solid particles are boosted by saline water in frazil slush. Solid particles are progressively gathered in solid inclusions while water is concentrated in brine droplets. A very rough estimate of the brine salinity may be made, assuming that the Cl contribution from solid solution may be neglected and that droplet distribution does not change significantly throughout ice sample: 5 droplets, 3 to 15 μm in size (Fig.5), have been observed in an area of 200 x 200 μm^2 with an investigation thickness of 50 μm. This corresponds to a distribution coefficient of ~ 10^{-3}, and a salinity of ~ 1.5 ‰ based on Cl concentrations in ice sample. This is significantly higher than the maximum salinity of 0.05 to 0.3 ‰ calculated for the main Lake [5] and supports the hypothesis of haline water provided by hydrothermal circulation [5]

The role played by grain boundaries seems to be of minor importance. Once formed, accreted ice remains very close to the melting point [3]. At high temperature (~-3°C), the minimization of grain boundary free energy implies abnormal grain growth associated with high crystalline quality of grain boundary structure [4]. At the beginning of grain growth process, grain boundaries likely gather thin particles. However, with progressive grain growth, particles aggregate and can be located in ice lattice. Considering its high salinity, brine is likely in liquid state at –3°C. Interaction between grain boundaries and liquid inclusions should be close to ice-water interaction, allowing brine bubbles to remain in ice lattice. The relaxation of water droplets during drilling, when the outer pressure decreases from 30 to 0.1 MPa, can initiate ice cracks along crystallographic plan, which could explain the form and orientation of bubble extensions visible in Fig.5. After drilling, at –50°C, brine droplets are expected to freeze leading to concentrations gradients as observed in brine bubbles (Fig.5), solute exclusion occurring at the ice water interface during the freezing process.

Both brine and mineral material are present in the particle studied in the ice-2 sample (S 3539, Fig.1) where sulfate salt and NaCl concentrations are very low (Table 1). The number and size of solid particles was probably very low, preventing aggregate formation and even gathering by grain boundary at the beginning of grain growth process. Cl mapping suggests that the salinity of brine water is much lower than in ice-1, which supports the sporadic occurrence of more saline water when ice-1 formed [5].

Conclusion

This preliminary work demonstrated that very useful information on impurities composition and localization in accreted ice from Lake Vostok may be inferred from XRF micro-analysis. This technique allowed to check previous hypothesis based on macroscopic chemical studies [5], in particular the existence of a sulfate salt rich reservoir and the occurrence of saline water pulses. Further investigations are required to go deeply into the nature, composition and origin of solid particles as well as the size and spatial distribution of brine droplets. More information on ice lattice and possible solid solution is also required.

REFERENCES:

1. A.P. Kapista, J.K. , G. de Q. Robin, M.J. Siegert, I.A. Zotikov, A large deep

freshwater lake beneath the ice of central East Antarctica, Nature 381 (1996) 684-686.

2. J.A. Dowdeswell, M.J. Siegert, The dimension and topography setting of Antarctic subglacial lakes and implications for large-scale water storage beneath continental ice sheets, GSA Bull. 111 2 (1999) 254-263.

3. J. Jouzel, J.-R. Petit, R. Souchez, N.I. Barkov, V.Ya. Lipenkov, D. Raynaud, M. Stievenard, N.I. Vassiliev, V. Verbeke, F. Vimeux, More Than 200 Meters of Lake Ice Above Subglacial Lake Vostok, Antarctica, Science 286 (1999) 2138-2141.

4. M. Montagnat, P. Duval, P. Bastie, B. Hamelin, O. Brissaud, M. de Angelis, J.-R. Petit, V.Ya Lipenkov, High crystalline quality of large single crystals of subglacial ice above Lake Vostok (Antarctica) revealed by hard X-ray diffraction, C. R. Acad. Sci. Paris, Earth. Planet. Sci. 333 (2001) 419-425.

5. M. De Angelis, J.R. Petit, J. Savarino, R. Souchez , and M.H. Thiemens, Contributions of an

   ancient evaporitic-type   reservoir to subglacial Lake Vostok chemistry, EPSL, in press.

6. M. Studinger, G.D. Karner, R.E. Bell, V. Levin, C.A. Raymond, A.A. Tikku, Geophysical models for a tectonic framework of the Lake Vostok region, East Antarctica, Earth Planet. Sc. Lett. 216 (2003) 663-677.

7. M.C Morel Fourcade, J.M.Barnola, J. Susini, G. Durand, M de Angelis and P. Duval, Application of micro X-ray fluorescence to impurity mapping of polar ice, J. Glaciol., submitted

8. M.C Fourcade, J.M.Barnola, J. Susini , R.Baker, XRF elemental mapping of polar ice, Poster, International Congress on X-Ray Optics and Microanalysis, Chamonix France (2003)

9. M. Legrand, M. de Angelis and F. Maupetit, Field investigations of major and minor ions along the Summit (central Greenland) ice cores using ion chromatography, J. Chromatogr. 640 (1993), 251-258.